Virology 527 (2019) 1–11

Contents lists available at ScienceDirect

Virology

journal homepage: www.elsevier.com/locate/virology

Identification of insect genes involved in baculovirus AcMNPV entry into insect cells

Jeffrey J. Hodgson[a], Nicolas Buchon[b], Gary W. Blissard[a,*]

[a] Boyce Thompson Institute at Cornell University, Tower Road, Ithaca, NY 14853, USA
[b] Department of Entomology, Cornell University, Ithaca, NY 14853, USA

ARTICLE INFO

Keywords:
Virus entry
Baculovirus
Drosophila
AcMNPV
Rab1
High throughput screen

ABSTRACT

The baculovirus *Autographa californica* multiple nucleopolyhedrovirus (AcMNPV) is a model enveloped DNA virus that infects and replicates in lepidopteran insect cells, and can efficiently enter a wide variety of non-host cells. Budded virions of AcMNPV enter cells by endocytosis and traffic to the nucleus where the virus initiates gene expression and genome replication. While trafficking of nucleocapsids by actin propulsion has been studied in detail, other important components of trafficking during entry remain poorly understood. We used a recombinant AcMNPV virus expressing an EGFP reporter in combination with an RNAi screen in *Drosophila* DL1 cells, to identify host proteins involved in AcMNPV entry. The RNAi screen targeted 86 genes involved in vesicular trafficking, including genes coding for VPS and ESCRT proteins, Rab GTPases, Exocyst proteins, and Clathrin adaptor proteins. We identified 24 genes required for efficient virus entry and reporter expression, and 4 genes that appear to restrict virus entry.

1. Introduction

Viruses are obligate intracellular pathogens that have evolved intricate mechanisms to deliver their genetic information into the appropriate compartment of a potential host cell. Bacteriophages may circumvent the protective cell wall of their bacterial host by injecting their genetic information directly into the cell. Some enveloped eukaryotic viruses fuse directly with the cell plasma membrane while others enter by cellular endocytosis. There are a variety of characterized mechanisms of endocytosis such as clathrin- or caveolae-mediated endocytosis, pinocytosis and phagocytosis, in addition to less well-understood cellular uptake events that do not fall specifically into any of these categories (Mercer et al., 2010). It is also possible that a single virus may enter the same or different cell types by different routes or mechanisms, perhaps depending on membrane composition or the presence of a particular cellular receptor. For many viruses, entry results from virion binding and clathrin-mediated endocytosis (Mercer et al., 2010, Hefferon et al., 1999; Long et al., 2006; Volkman and Goldsmith, 1985). Endocytosed virus particles are contained within early endosomes, which tether to and transit along cytoskeletal elements with the aid of a variety of regulatory proteins such as Rab GTPases. Such proteins direct and regulate subcellular locomotion needed for vesicle interaction and/or merging with late endosomes, autophagosomes or lysosomes. For many enveloped viruses, the acidification that occurs within the maturing early or late endosome activates a viral membrane fusion protein (or complex) such that viral nucleocapsids are released from endocytic vesicles prior to their merging with lysosomes or autophagosomes which typically would result in degradation of the incoming viral particles and thus would block cellular infection.

Large DNA viruses such as baculoviruses, iridoviruses, and herpesviruses transcribe and replicate their genomes in the host cell nucleus. Therefore, for these viruses successful entry requires trafficking to the nucleus. Virus binding, uptake and transport to the necessary subcellular compartment are all critical steps that determine the success of virus infection at the cellular level. Identifying key cellular processes that govern entry and the initiation of infection will provide targets for strategies to either block viral infection of new host cells or to enhance susceptibility of cells to productive viral infection. In the latter case, enhanced entry could improve virus-based gene delivery or increase therapeutic protein production when viral vectors are used. Inhibition of cellular factors that restrict virus infection might also expand the host-range or otherwise enhance host insect susceptibility to viruses used for biological pest control.

Baculoviruses are large DNA viruses that infect insects. They have been used successfully as biological control agents, and have been developed as an important eukaryotic protein expression system for many biotechnological applications. Baculoviruses also represent an

* Corresponding author.
E-mail addresses: jjh364@cornell.edu (J.J. Hodgson), nicolas.buchon@cornell.edu (N. Buchon), gwb1@cornell.edu (G.W. Blissard).

https://doi.org/10.1016/j.virol.2018.10.022
Received 9 August 2018; Received in revised form 19 October 2018; Accepted 21 October 2018
Available online 13 November 2018
0042-6822/ © 2018 Elsevier Inc. All rights reserved.

emerging platform for the production of gene therapy vectors (Felberbaum, 2015; Hu, 2010; Kalesnykas et al., 2017). The budded form of the baculovirus virion binds and enters many cell types (even cells that are not permissive for viral replication) and delivers the genome to the nucleus, albeit at varying efficiencies for unknown reasons. Baculovirus budded virions bind an unknown receptor and are taken up into both permissive insect and non-permissive mammalian cells by clathrin-mediated endocytosis (Airenne et al., 2013; Dong and Blissard, 2012; Hefferon et al., 1999; Long et al., 2006; Wang et al., 1997; Wickham et al., 1990, 1992). Budded virions of the model baculovirus, AcMNPV, display a class III envelope fusion protein called GP64, which binds the cellular receptor. Following internalization of the virion, the endosome is transported and incrementally acidified. After a critical pH is achieved within the endosome, a conformational change in GP64 occurs, resulting in membrane fusion activity by the GP64 protein and fusion of the virion envelope and endosome membrane. Following release into the cytoplasm, the nucleocapsid is subsequently trafficked to the nucleus via a propulsion system that involves F-actin polymerization for nucleocapsid movement and transit through the nuclear pore (Au et al., 2016; Mueller et al., 2014; Ohkawa et al., 2010; Ohkawa and Welch, 2018). Within the nucleus, the nucleocapsid uncoats and the viral DNA genome is released and early gene expression proceeds.

In the current study, we used an RNAi knockdown approach to identify cellular factors that impact AcMNPV uptake. For these studies, we used a recombinant AcMNPV baculovirus encoding a nuclear-localized EGFP (NLS-EGFP) reporter gene in combination with *Drosophila* DL1 cells, which are highly amenable to dsRNA mediated RNAi but are non-permissive for viral replication. We targeted 86 candidate genes: genes involved in aspects of subcellular vesicular transport and thought to be involved in entry by viruses. Candidate genes for knockdowns included 27 Rab GTPases (including *Rab5* and *Rab7*, both of which are essential for endosome acidification), vacuolar protein sorting (Vps) genes, clathrin and exocyst complex components, several ESCRT pathway genes, and other selected genes. We identified 28 genes that had significant effects on detection of the reporter. Of these 28 genes, 24 reduced reporter detection by at least 35%, and four (*Rab1*, *Vps2*, *Sar1*, *betaCOP*) increased reporter detection from 2 to 10 fold. Because a knockdown of *Rab1* mRNA enhanced reporter activity by more than 10-fold, we examined potential effects of the *Rab1* knockdown on early events in entry. We found that neither binding nor the initial internalization of AcMNPV was substantially enhanced by RAB1 depletion, suggesting that the effect of *Rab1* knockdown occurs after the virus binds and is internalized into the endosome, and likely affects endosomal trafficking or actin-mediated propulsion.

2. Materials and methods

2.1. Cells and viruses

Drosophila DL1 cells were grown in Schneider's medium (Invitrogen) supplemented with 10% Fetal Bovine Serum (FBS, Hyclone). *Spodoptera frugiperda* Sf9 cells were grown in Supplemented Grace's Medium (Invitrogen Cat. No. 11605) containing 2.5% FBS, 1x penicillin/streptomycin (Invitrogen) and 0.1% pluronic acid F-68.

For construction of the reporter virus, the *Drosophila* actin promoter was first PCR amplified and cloned into a pFastbac dual vector in the orientation of the *polh* promoter in a manner that excised the back-to-back *p10* and *polh* promoters. This plasmid was named pFBactin-Linker. The *egfp* gene was cloned downstream of the *Drosophila actin* promoter to generate pFBactin:NLS-EGFP, which was subsequently used to generate a bacmid (AcGFP) by standard methods (O'Reilly et al., 1992). Bacmid AcGFP was transfected into Sf9 cells and the resulting virus was amplified, then stored at 4 °C. The baculovirus used for qPCR analysis of binding and endocytosis was generated using a pFBactin-Linker transfer vector that contained the AcMNPV *gp64* ORF downstream of the *Drosophila actin* promoter (pFBactin-GP64).

2.2. dsRNA synthesis and RNAi Knockdowns

DNA templates for T7 RNA polymerase synthesis of gene-specific dsRNAs were purchased from the *Drosophila* Screening Resource Center (DSRC) at Harvard Medical School. The gene specific amplicons are listed in Table S1. DNA templates contain a 5′ T7 promoter on each strand for synthesis of dsRNA. Amplicons were amplified using Taq polymerase (Invitrogen) and a T7 primer (T7proFor: 5′ AAATTTAATACGACTCACTATAGGG 3′, T7 promoter is underlined). The PCR amplicons were used directly for dsRNA syntheses by adding 2 µl of each PCR reaction to 10 µl or 20 µl of an in vitro T7 transcription reaction (Cellscript). T7 transcription was performed at 37 °C for 12–16 h. Afterward, 0.5 µl of kit-supplied RNAase-free DNase was added and incubated at 37 °C for 1 h. dsRNAs were purified on Qiagen RNeasy mini columns, eluted in water and quantified by $OD_{260/280}$ measurement on a Nanodrop spectrophotometer. To produce larger quantities of dsRNA, the above transcription reactions were scaled ten-fold and dsRNAs were purified by phenol: chloroform extraction and ethanol precipitation.

For RNAi knockdowns in DL1 cells, 700 ng of each dsRNA in 15 µl of water was added to a well of a 96 well plate. Each dsRNA was added to three replicate wells. Controls included wells lacking dsRNA and wells seeded with a nonspecific lacZ dsRNA. Controls to monitor the efficiency of the RNAi mediated knockdown in each experiment included dsRNAs targeting *egfp* and *diap1* (which results in cell death when DIAP1 is depleted). *Drosophila* DL1 cells were grown to confluence in Schneider's medium + 10% FBS, in T25 flasks. Growth medium was removed from the flask and replaced with 3 ml serum-free Schneider's medium. The cells were dislodged into the serum-free medium and counted on a hemocytometer. Forty thousand cells in 30 µl serum-free medium was added to each well containing the dsRNA in water, and the plate was gently tapped to mix the dsRNA and cells before the plate was briefly centrifuged (1000 rpm for 30 s) to produce an even monolayer. Cells plus dsRNA were incubated for 30 min at RT, then 55 µl of Schneider's medium supplemented with 20% FBS was added to each well. The plates were then incubated in air-tight bags at 22 °C for 3 days. A dsRNA against the *Drosophila* inhibitor of apoptosis 1 (*diap1*) was included to monitor progression of RNAi for each batch of cells in replicate experiments. Knockdown of *diap1* resulted in the induction of apoptosis and cell death. After 3 days of dsRNA exposure, the AcGFP baculovirus was added to wells. A dsRNA against *egfp* (to knockdown the reporter virus expressed NLS-EGFP) was also incorporated as another control for assessing the robustness of RNAi by flow cytometry in replicate experiments. The amount of AcGFP added to wells was predetermined (see below) by diluting the stock virus in Sf9 cell growth medium (Supplemented Grace's Medium containing 2.5% FBS) and assessing expression of the EGFP reporter. A volume of 50 µl of the diluted AcGFP virus (which does not replicate in DL1 cells) was added to each well.

For follow-up studies of *Sar1* and *Rab1* knockdowns, cells were incubated with dsRNA for 5 days then re-plated at 2×10^5 cells per well (in 100 µl fresh medium) in triplicate wells of 96 well plates. Cells were allowed to attach and form monolayers for 2 h, then 10 µl of the AcGFP reporter virus was added to each well with gentle mixing. At 16 h post virus inoculation, cells were analyzed by flow cytometry for EGFP expression as described above. To confirm *Rab1* mRNA depletion in the follow-up RNAi protocol, we performed quantitative reverse transcriptase PCR on *Rab1* mRNA in Rab1 dsRNA and lacZ dsRNA treated cells. *Rab1* mRNA levels were reduced by approximately 90% relative to that from control cells treated with lacZ dsRNA.

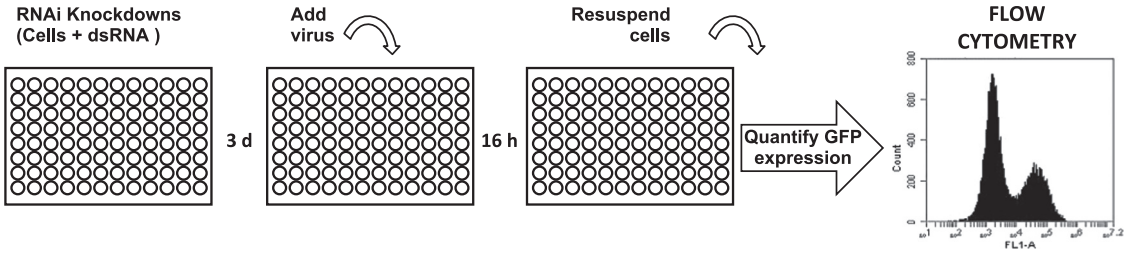

Fig. 1. The graphic shows the experimental design of the RNAi screen for effects of host gene knockdowns on reporter baculovirus (AcGFP) entry. DL1 cells were incubated with individual dsRNAs for 3 days in a 96-well plate format. The AcGFP reporter baculovirus was added to each well, incubated for 16 h, then cell density, total EGFP fluorescence levels, and the proportions of EGFP-positive cells were measured by flow cytometry.

2.3. Reporter virus entry screen

The dose of the AcGFP reporter virus used for transduction in RNAi assays was determined empirically by inoculating DL1 cells with a range of 2-fold dilutions of the virus stock. A 5-fold dilution of the AcGFP stock virus preparation was used for these assays since that dilution resulted in maximal transduction (5–10%) of untreated cells. The virus inoculum was added to the 100 µl of Schneider's growth medium on the cells and mixed (by gently pipetting 5×). At 16 h post-inoculation, the virus and growth medium were removed and cells from each well were re-suspended in 100 µl of PBS (pH 7.4), then analyzed by flow cytometry (Accuri C6) for EGFP expression (Fig. 1). Cell samples were assessed for both the number of EGFP positive cells and the intensity of the mean fluorescence of the EGFP positive cell population. For analysis of the effects of RNAi knockdowns, assessments were based on the proportion of EGFP positive cells as the readout for EGFP detection. EGFP measurements for all RNAi treated cells were normalized relative to that of control lacZ RNAi treated cells (Table S3). To identify any potential negative effects of specific dsRNA knockdowns on cell viability, total cell numbers were also monitored. The knockdowns of *Vps2*, *Vps4*, *Vps32, Rab5,* and *betaCOP* resulted in reduced cell numbers (i.e. less than 50% of that from lacZ dsRNA treated cells) (Fig. 2c), and were therefore considered to be toxic to the cells. For the analysis of virus entry, EGFP values were based on the proportion of EGFP positive cells normalized to the values for lacZ dsRNA treated wells on each plate. To assess the effects of each dsRNA on reporter virus uptake, we calculated the mean of the lacZ normalized values for three replicate wells per assay, and performed at least three iterations of independent experiments (Fig. 2a). We calculated a z-factor, a value used to evaluate the statistical effect size for our assay, based on the EGFP positive cell proportions of all 86 knockdowns of the initial RNAi screen dataset. The calculated z-factor (equal to 0.676) indicated that the screen was able to identify significant effects on reporter virus activity due to RNAi knockdowns (Zhang et al., 1999). To help define significant effects influenced by the individual gene knockdowns we performed ANOVA (Dunnett's test; Graphpad Prism 7.0). The ANOVA analysis for the entire dataset is listed in Table S2. Table 1 summarizes the 28 RNAi knockdowns that yielded significant hits from the screen. Robust z-scores (Z′) insensitive to outliers common to RNAi screens (Birmingham et al., 2009), based on the median absolute deviations obtained for replicate assays of each knockdown, were also calculated for individual gene knockdowns (see Table S3) to qualify our assignment of “hits” from this assay.

To subsequently assess with more precision, the effects of selected gene knockdowns on AcMNPV binding and internalization, a “scale-up” protocol was used for RNAi. Cells (15×10^6 cells in 0.7 ml or 40×10^6 cells in 1.3 ml of serum-free medium) were exposed to 21 µg or 55 µg of dsRNA in 35 mm or 60 mm dishes, respectively, for 30 min at RT. After the initial 30 min incubation, 1 ml (35 mm dish) or 2 ml (60 mm dish) of Schneider's medium containing 20% FBS was added and dishes were sealed with parafilm and incubated at 22 °C for 5 days.

2.4. Phagocytosis assay

Cells treated with selected dsRNAs were also assessed for effects on cellular phagocytosis. Cells were treated with dsRNAs as described above. At 3 days post dsRNA exposure, growth medium was aspirated from wells and replaced with 50 µl of the pHrhodo Red *E. coli* bioparticle (Invitrogen) phagocytosis reagent (0.5 mg/ml) in Schneider's medium containing 10% FBS, then incubated at 27 °C for 30 min. Plates were then placed on ice and cells were subsequently resuspended in PBS (pH 7.4) and analyzed by flow cytometry (Accuri C6) for the presence of red fluorescence as a marker of bacteria internalized and reaching the phagolysosome.

2.5. Virus binding assay

For AcMNPV binding assays, 200 ml of AcMNPV BV from cell culture supernatant was first concentrated by ultracentrifugation (75 min at 80,000×*g*, 4 °C) through a 25% sucrose pad, and the pellet was re-suspended in 500 µl of 1x DNAse I buffer. To remove free viral DNA, 20 units of RQ1 DNAse (Promega) was added to the virus suspension and incubated at 37 °C for 15 min. Aliquots of the resulting virus preparation were stored at −20 °C, and diluted immediately prior to each binding experiment. A range of dilutions of the virus preparation was examined in binding assays on *Drosophila* DL1 cells to establish a dilution that permitted quantitative PCR detection of the viral genome in a linear range of detection.

Cells were exposed to dsRNA for 5 days at 22 °C as described above for the RNAi scale-up. Cells were then re-suspended and gently pelleted by centrifugation (5 min at 1000 x *g*). Cell pellets were re-suspended in 0.3 ml Schneider's medium containing 1% FBS, counted with a hemocytometer, and diluted to 3 million cells/ml in the same medium. Aliquots (50 µl) of the cell suspension were chilled on ice for 30 min, then 50 µl of the virus preparation (diluted in the same medium) was added to each tube. Cells and virus were initially, and intermittently (every 20 min) mixed by gentle vortexing. Cell/virus mixtures were incubated on ice for 1 h, then cells were washed 3x with cold PBS (pH 7.4) by centrifugation (1000 x *g*, 5 min at 4 °C) and re-suspension in 1 ml of PBS. Washed pellets were then stored at −20 °C until total DNA (cell + virus) was purified using Qiagen DNeasy Blood and Tissue columns (cultured cell protocol). DNA was eluted into 30 µl of the kit elution buffer, quantified (Nanoview, GE), adjusted to 3 ng/µl in water, and stored at −20 °C. Two replicate tubes of cells were tested in this manner for each experiment, and the experiment was repeated three times.

2.6. Virus endocytosis assay

After 5 days of dsRNA exposure, cells were collected and counted as described for the binding assay, except that the collected cell pellets were re-suspended in Schneider's medium containing 10% FBS. Cells were seeded (1.5 million cells/well) into a 24-well plate and allowed to attach at RT for 1 h, then the plate was centrifuged at 1000 x *g* for 5 min

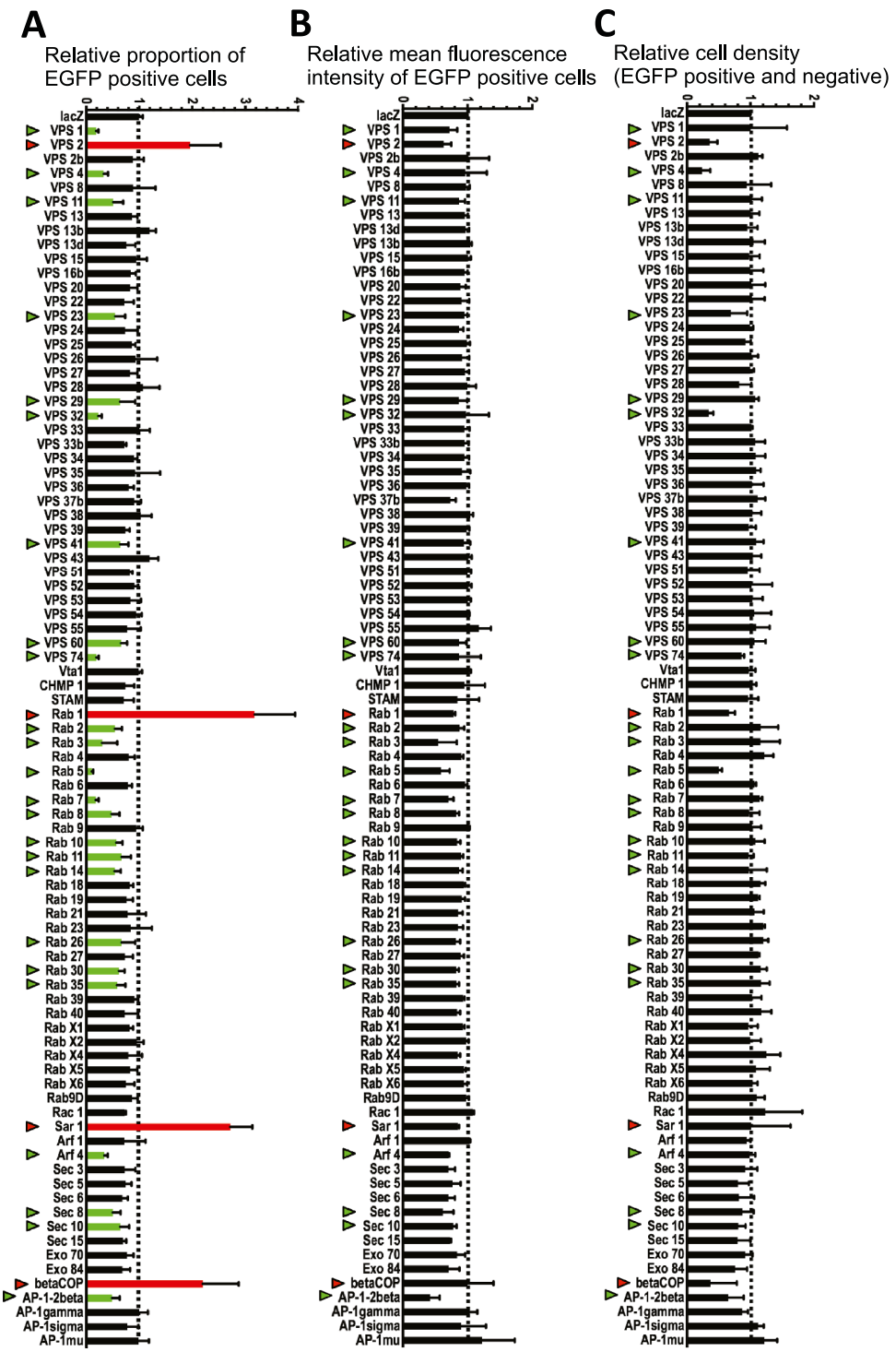

Fig. 2. Results of RNAi knockdowns of host genes on reporter (NLS-EGFP) detection from the reporter baculovirus (AcGFP) in the viral entry screen. For each graph, host DL1 genes targeted for RNAi are listed on the left. In each graph, the dashed line indicates the baseline detected for control cells treated with lacZ dsRNA. The 24 gene knockdowns that significantly reduced reporter EGFP detection are indicated by green arrowheads on the left of each graph. The 4 gene knockdowns that significantly increased reporter EGFP detection are indicated with red arrowheads. **A)** Relative proportion of EGFP-positive cells. **B)** Relative mean fluorescence intensity of EGFP-positive cells. **C)** Relative cell density of EGFP-positive and –negative cells (cell viability) as a measure of toxicity of dsRNA treatments. The 28 gene knockdowns that significantly altered EGFP detection are summarized in Table 1.

at 22 °C and incubated for 1 additional hour at RT. The medium in each well was replaced with 500 µl cold (4 °C) Schneider's medium containing 1% FBS, and the plates were incubated on ice for 30 min. For the endocytosis assays, the concentrated virus preparation used for the binding assays was further diluted 50-fold in PBS (pH 7.4) and filtered through a 0.45 µm PES filter to remove any large aggregates of virus particles, aliquoted, and thawed just prior to performing the endocytosis assay. The filtered virus preparation was thawed and diluted 5-fold in cold Schneider's medium containing 1% FBS and 150 µl was used to replace the medium on cells in each well of the pre-chilled plates, and incubated on ice for 1 h to allow virus binding to cells. After a 1 h incubation on ice, excess unbound virus was removed from cell monolayers by washing (3×) with 0.5 ml of cold PBS (pH 7.4). After the washes, 0.5 ml of prewarmed (27 °C) Schneider's medium containing 10% FBS was added to each well and plates were then incubated at 27 °C for 1 h to permit virus endocytosis. A duplicate plate of the cell/virus combination was kept on ice for 1 h with 0.5 ml of ice-cold Schneider's medium plus 10% FBS after the PBS washes to serve as a control for removal of extracellular virus particles by trypsinization. After the 1 h incubation (on ice or at 27 °C) media from each well was aspirated and monolayers were rinsed 1x with RT PBS, followed by addition of 0.5 ml of prewarmed (37 °C) trypsin (0.25%, Invitrogen) to

Table 1
Summary of significant RNAi hits.

		Gene[1]	% EGFP Positive Cells	P-Value[2]	% Cell Density
Important for virus entry[3]	Strongly Inhibitory Knockdown	Rab 5	10.5	<0.0001	50.0
		Rab 7	18.5	<0.0001	114.6
		VPS 1	19.2	<0.0001	100.6
		VPS 74	19.6	<0.0001	85.7
		VPS 32	22.9	<0.0001	34.4
		Rab 3	30.5	<0.0001	116.0
		VPS 4	33.2	<0.0001	24.3
		Arf4	34.5	<0.0001	98.8
	Moderately Inhibitory Knockdown	Rab 8	48.1	<0.0001	98.4
		AP-1-2beta	49.0	<0.0001	65.1
		Sec 8	50.6	<0.0001	87.5
		VPS 11	51.4	<0.0001	102.4
		Rab 14	54.1	0.0002	97.8
		Rab 2	54.4	0.0003	116.4
		VPS 23	54.9	<0.0001	69.2
		Rab 10	57.3	0.0009	108.3
		Rab 35	58.3	0.0015	117.1
	Weakly Inhibitory Knockdown	Rab 30	62.2	0.019	116.4
		VPS 29	64.2	0.005	107.9
		Sec 10	64.3	0.0052	81.1
		VPS 41	64.4	0.0054	109.2
		VPS 60	66.0	0.0102	106.8
		Rab 11	66.8	0.0347	97.5
		Rab 26	66.9	0.0358	120.5
Restrict[4] virus entry	Stimulatory Knockdown	Rab 1	317.6	<0.0001	66.9
		Sar 1	271.5	<0.0001	101.1
		betaCOP	219.8	<0.0001	37.5
		VPS 2	196.2	<0.0001	35.7

1 Genes are listed in descending order of their extent of altering EGFP detection seen in gene knockdowns.
2 P-values are based on a Dunnett's test.
3 Knockdowns causing less reporter EGFP detection are regarded to promote virus entry.
4 Knockdowns that enhance reporter EGFP detection are considered as restrictive for virus entry.

each well. Plates were incubated at 37 °C for 10 min, then cells from monolayers were re-suspended by pipetting with a P1000 micropipette, and then pelleted by centrifugation (1000 × *g*, 5 min at 4 °C). Cells were washed three times to remove any extracellular virus, by re-suspending cell pellets in 1 ml PBS (by gentle vortexing) then pelleting. Washed cell pellets were stored at −20 °C until total DNA (cell + virus) was isolated with the Qiagen DNeasy Blood and Tissue columns (cultured cell protocol). DNA was eluted in 30 µl of kit elution buffer, quantified with a Nanoview (GE), diluted to 3 ng/ul in water and stored frozen at −20 °C until used for qPCR.

A range of 2-fold dilutions of the filtered virus preparation was added to lacZ dsRNA-treated *Drosophila* DL1 cells to assess quantitative detection of internalized viral genomes in this qPCR assay. We observed a linear response in detectable AcMNPV internalization over an eight-fold range of the AcMNPV virus inoculum. A 5-fold dilution was used for the endocytosis assay. Two-fold dilutions of the filtered virus preparation (as used for determining the appropriate dose for the endocytosis assay) were also included in parallel for each endocytosis assay with lacZ dsRNA-treated cells to confirm quantitative virus detection in each iteration of the experiment (Fig. 5B).

2.7. Quantitative PCR

Total DNA measured in virus binding and endocytosis assays was measured as the ratio of viral DNA: cell DNA. For these measurements, we used the AcMNPV the *ODVe56* gene (forward: 5′-GATCTTCCTGCG GGCCAAACACT-3′; reverse: 5′-AACAAGACCGCGCCTATCAACAAA-3′) (Li and Blissard, 2012) and the *Drosophila Rp49* (or *RpL32*) gene (Forward: 5′-GACGCTTCAAGGGACAGTATCTG-3′, Reverse: 5′-AAACGCGG TTCTGCATGAG-3′) for quantitative PCR. Virus levels relative to reference were calculated by the formula: $(Rp49_{eff}{}^{\hat{}Ct_Rp49ct})/(virus_{eff}{}^{\hat{}Ct_virus})$ where the eff and Ct subscripts refer to the primer efficiency (eff) and cross-threshold (Ct).

2.8. RT-qPCR

RNA extracted from lacZ, Rab1 or Atg1 dsRNA-treated cells was isolated with Qiagen RNeasy mincolumns. Five units of RQ1 DNase (Promega) was used to treat 5 µg of each RNA sample prior to reverse transcription. One ug of each RNA was reverse-transcribed using Superscript III (Invitrogen) with oligoDT (Invitrogen) according to the manufacturers instructions. A reaction containing no reverse transcriptase was carried out for each RNA sample and carried through the qPCR to confirm the absence of contaminating genomic DNA in RNA samples. The *Rp49* qPCR primers were the same as those used for total DNA qPCR described above. The following additional primers were also used: Rab1 (Forward: 5′-CCTGTCTTCTGTTGCGATTTGCCG-3′, Reverse: 5′CTCCTGGCCAGCAGTATCCC-3′) and Atg1 (Forward: 5′-GCGCGATT CCTGAACGAGGG-3′, Reverse: 5′-CTGGTAGACAATCGTTCCCAGCG-3′). Gene levels relative to the reference were calculated by the formula: $(Rp49_{eff}{}^{\hat{}Ct_Rp49ct})/(gene_{eff}{}^{\hat{}Ct_gene})$ where the eff and CT subscripts refer to the primer efficiency (eff) and cross-threshold (Ct).

2.9. Western Blots

For western blot analysis to confirm ATG8 depletion upon *Atg8a* knockdown, cells exposed to control lacZ or *Atg8a*-specific (DRSC18024) dsRNAs for 4 days were collected and lysed in a buffer (10 mM tris-HCl, 100 mM NaCl, 1% triton-x 100; pH 8.0) containing a protease inhibitor cocktail (Roche). Proteins were separated by SDS-PAGE (12%) and transferred to a PVDF membrane. A single blot was bisected horizontally to separate the low and high molecular weight proteins of each sample to enable simultaneous immunodetection of ATG8 and the GAPDH loading control. ATG8 was detected (Invitrogen NBT/BCIP) with rabbit anti-ATG8a (Takats et al., 2013) (1:3000) and GAPDH was detected with rabbit anti-GAPDH GeneTex (1:5000, GTX100118) and an alkaline phosphatase conjugated anti-rabbit

antibody (Sigma). Blots were photographed and optimized for brightness and color in Powerpoint.

3. Results

3.1. Effects of cellular gene knockdowns on baculovirus entry

The budded virus (BV) form of the baculovirus, AcMNPV, enters and traffics to the nucleus of many heterologous cell types. Because of this characteristic, AcMNPV BV is used widely as a transduction vector (Airenne et al., 2013; Mansouri et al., 2016; Mansouri and Berger, 2018). The cellular requirements for virus trafficking during entry are poorly understood for this and other viruses. To identify cellular proteins and pathways that are involved in entry of AcMNPV BV, and perhaps other enveloped viruses, we developed an RNAi-based semi-high-throughput screen for virus entry in *Drosophila melanogaster* DL1 cells (Fig. 1), an insect cell line that is non-permissive for AcMNPV replication. While host gene knockdowns using RNAi are possible in permissive lepidopteran cell lines, we found that lepidopteran cells require transfection reagents for dsRNA mediated knockdown and that dsRNA transfection efficiencies may be highly variable (unpublished observations). The use of the DL1 cell line for RNAi has been extensively documented, requires no transfection reagents (dsRNAs are readily imported into DL1 cells), and is highly efficient (Yasunaga et al., 2014). For entry screens, the replication of the viral vector may also complicate the interpretation of the results since knockdowns that affect DNA replication may affect reporter gene expression due to variations in template copy number. The AcMNPV baculovirus does not replicate in DL1 cells and thus, use of the DL1 system avoids misinterpretation due to effects of knockdowns on events downstream of viral entry and gene expression. An additional advantage of the DL1 cell system is the availability of a vast pan-genomic array of RNAi amplicons that are available through the Drosophila RNAi Screening Center (DRSC, https://fgr.hms.harvard.edu/), reagents which must be developed gene by gene for each lepidopteran host species. To assess the effects of host gene knockdowns on virus entry, we challenged DL1 cells with a recombinant AcMNPV virus (AcGFP) containing an EGFP reporter gene (NLS-EGFP) under the control of a *D. melanogaster actin* promoter. Because AcGFP does not replicate in DL1 cells, quantification of reporter gene expression was used as a measure of virus entry and trafficking to the nuclei of infected cells.

We selected a variety of host genes with known roles in vesicular transport for analysis by RNAi knockdowns (Table S1, Fig. 2). For gene knockdowns, *Drosophila* DL1 cells were first incubated with individual dsRNAs for 3–4 days, then inoculated with the reporter virus (AcGFP). Cells and virus were then incubated for 16–24 h, and cell viability and EGFP levels were measured by flow cytometry. To control for general effects of dsRNA on DL1 cells, a non-specific dsRNA (targeting the *lacZ* gene) was used as a control and EGFP levels in the presence of each cellular gene knockdown were measured against that of the lacZ dsRNA knockdown control. To determine which effects were significant, we performed ANOVA (using a Dunnett's test) for the entire set of 86 dsRNAs (Table S2). We then categorized gene knockdowns, according to the relative degree of change in EGFP reporter detection. The results from the analysis of 86 genes are summarized in Fig. 2 and Table S3.

Of the 86 gene knockdowns, we identified 28 that consistently and substantially altered reporter EGFP levels (Fig. 2A, triangles; Table 1), suggesting effects on entry. Knockdown of *Rab5* resulted in the most dramatic reduction of EGFP reporter activity. Prior studies have shown that RAB5 depletion blocks endosomal maturation (inhibiting acidification of the endosome) which is required for viral membrane fusion and release of nucleocapsids into the cytoplasm (Kukkonen et al., 2003; Liu et al., 2014). Thus, the *Rab5* knockdown also served as a positive control for RNAi knockdown effects on virus uptake in follow-up experiments. Among the gene knockdowns that resulted in the most significant effects on EGFP detection, we subdivided the effects into 4 categories based on both the percent reduction in EGFP detection and the statistical significance (p-value) determined by ANOVA (Table 1). The four categories are: Strongly inhibitory, Moderately inhibitory, Weakly inhibitory, and Stimulatory. Of the 24 genes that resulted in reduced reporter levels (Fig. 2A, green bars), the 8 gene knockdowns that caused the greatest reductions (strongly inhibitory) in virus entry as measured by EGFP fluorescence ($\leq$ 35% of control) included *Rab5*, *Rab7*, *Vps1*, *Vps74*, *Vps32*, *Rab3*, *Vps4*, *Vps74*, and *Arf4*. Gene knockdowns that caused moderate decreases in EGFP levels (48–58% of control) included *Rab8*, *AP-1–2beta*, *Sec8*, *Vps11*, *Rab14*, *Rab2*, *Vps23*, *Rab10* and *Rab35*. The gene knockdowns that caused weak but significant reductions (59-67% of control) included *Rab30*, *Vps29*, *Sec10*, *Vps41*, *Vps60*, *Rab11* and *Rab26*.

Because cells were incubated for 3–4 days with dsRNAs and some knockdowns may affect cell growth, we also assessed the effect of each gene knockdown on growth and proliferation of cells (Fig. 2C). For most genes examined, dsRNA knockdowns did not severely affect cell growth (Fig. 2C; dashed line). RNAi knockdowns were considered toxic if the cell density was reduced to less than 50% of that from control lacZ dsRNA treated cells. We identified 5 gene knockdowns that substantially altered cell growth and/or viability (Fig. 2C; *Vps2*, *Vps4*, *Vps32*, *Rab5*, and *betaCOP*).

Perhaps most interesting and significant, we found that knockdowns targeting four genes (*Rab1, Vps2, betaCOP,* and *Sar1*) resulted in an increase (approximately 2- to 3-fold) in EGFP positive cells suggesting that these gene products may restrict virus entry (Fig. 2A, red bars). Each of these four knockdowns resulted in at least a 2-fold increase in EGFP reporter detection relative to that observed in control lacZ dsRNA treated cells. *Vps2* and *betaCOP* knockdowns caused $\geq$ 2-fold increases in reporter EGFP detection, and *Rab1* and *Sar1* knockdowns caused $\geq$ 2.7-fold increases in reporter EGFP detection (Table 1). We also noted that although the knockdown of both *betaCOP* and *Vps2* appeared to increase the percentage of EGFP positive cells (Fig. 2A), these knockdowns also resulted in reduced growth of cells (Fig. 2C) raising the possibility of pleiotropic effects.

3.2. Phagocytosis was not enhanced by the knockdown of Rab1, Vps2, Sar1 or betaCOP

Because the knockdowns of *Rab1*, *Vps2*, *Sar1*, and *betaCOP* increased reporter EGFP detection, this suggested that these proteins could limit viral entry or trafficking and we further examined their effect on cellular physiology. As it has been previously reported that DL1 cells and other hemocyte-like *Drosophila* cell lines are naturally phagocytic (Cherry, 2008), we first asked whether these knockdowns also increased cellular uptake levels by phagocytosis. To determine whether these four RNAi knockdowns induced a general increase in phagocytosis, we measured phagocytosis activity in the presence of *Rab1, Vps2, Sar1* and *betaCOP* knockdowns, using pHrhodo conjugated *E. coli*, which fluoresces following phagocytosis when reaching the low pH of the phagolysosome. RAB5 is needed for early endosome acidification and therefore knockdown of *Rab5* is expected to decrease fluorescence of pHrhodo conjugated *E. coli*. Thus, a *Rab5* knockdown was included as a control for this assay. As anticipated, cells with a *Rab5* knockdown elicited very little fluorescence confirming that RAB5 is important for phagocytosis. In comparison to the lacZ control RNAi knockdown, we detected no increase in phagocytosis for the *Rab1, Vps2, Sar1,* or *betaCOP* RNAi knockdowns (Fig. 3), which all enhanced AcGFP reporter activity in the entry screen (Fig. 2A). Furthermore, except for the *Rab1* knockdown (which showed no substantial effect on phagocytosis), gene knockdowns of *Vps2*, *Sar1* and *betaCOP* resulted in lower levels of detected phagocytosis. Therefore, the enhanced virus entry and reporter expression that we observed in the presence of the *Rab1*, *Vps2*, *Sar1* and *betaCOP* knockdowns was not due to a general increase in phagocytic uptake, but rather appears to be specific to entry by the virus particles. We also noted that most, but not all of the 24

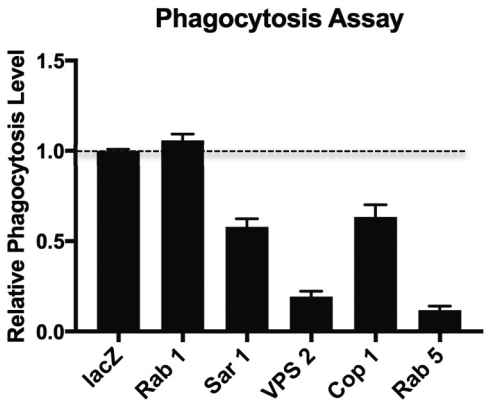

Fig. 3. Effects of selected gene knockdowns on phagocytic activity of DL1 cells. Levels of phagocytosis in cells exposed to the indicated dsRNAs and treated with a pH sensitive dye conjugated to *E. coli* (pHrhodo), were measured by flow cytometry. Phagocytosis levels were assessed relative to that from control cells incubated with lacZ dsRNA (lacZ, dashed line).

RNAi knockdowns that significantly inhibit baculovirus entry, also reduced phagocytosis using this same assay (see Fig. S1).

3.3. Confirmation of enhanced virus entry

In the initial screen, we identified four genes that appear to restrict virus entry. To confirm and more carefully examine this effect, we modified the RNAi analysis protocol to improve comparisons. For the initial 96-well based semi-high-throughput RNAi screen, cells exposed to some dsRNAs for prolonged periods grew in foci or at different rates. To insure equivalent accessibility of cells to the reporter baculovirus and to enhance knockdowns, cells were treated with dsRNA for 5 days then detached, re-suspended, and re-plated at equal cell densities to form even monolayers prior to adding the reporter baculovirus. Using the same reporter baculovirus (AcGFP), we observed similar levels of enhancement for *Sar1* (Fig. 4) as was observed previously (Fig. 2A). However, using the modified approach, the *Rab1* RNAi knockdown resulted in a more than 10-fold increase in EGFP positive cells relative to the lacZ dsRNA treated control cells (Fig. 4B). As expected, we detected little EGFP in the control *Rab5* knockdown cells. Cells in which either *Vps2* or *betaCOP* were targeted for knockdown did not efficiently re-attach to culture plates as required in the modified assay, and therefore *Vps2* and *betaCOP* were not further assessed.

3.4. Knockdown of Rab1 does not enhance AcMNPV binding to cells

We found that a *Rab1* knockdown resulted in enhanced EGFP reporter detection in AcMNPV infected cells, suggesting enhanced entry in the absence of RAB1. Because RAB1 has previously been described as playing a variety of roles in the cell (including regulation of ER-Golgi and intra-Golgi trafficking, autophagy-related membrane-tethering events, and actin polymerization) (Barrowman et al., 2010; Russo et al., 2016), we reasoned that the *Rab1* knockdown may affect one or more of the steps in virus entry, such as: binding at the surface, internalization into an initial endosome, transit of the endosome, release from the endosome, actin-mediated transport, or even nuclear entry. Therefore, we first asked whether the binding of AcMNPV at the cell surface was affected by the *Rab1* knockdown. To examine virion binding, we used qPCR to detect quantitative changes in virus particles bound to the surface of cells treated with either Rab1 or control lacZ dsRNA (Fig. 5A). We also assessed virus binding to Rab5 dsRNA treated cells since knockdown of *Rab5* caused the most drastic reduction in reporter EGFP detection in all our prior experiments. To first confirm quantifiable detection of virus binding at the cell surface, we first showed that AcMNPV DNA could be detected by qPCR, in a dose-dependent manner, from AcMNPV BV bound to the cells. A BV dose within the linear range of the qPCR assay was selected for binding experiments. For this assay, AcMNPV BV was bound to cells on ice (which inhibits endocytosis) for 1 h, then cells were washed (on ice) to remove unbound virus. Total

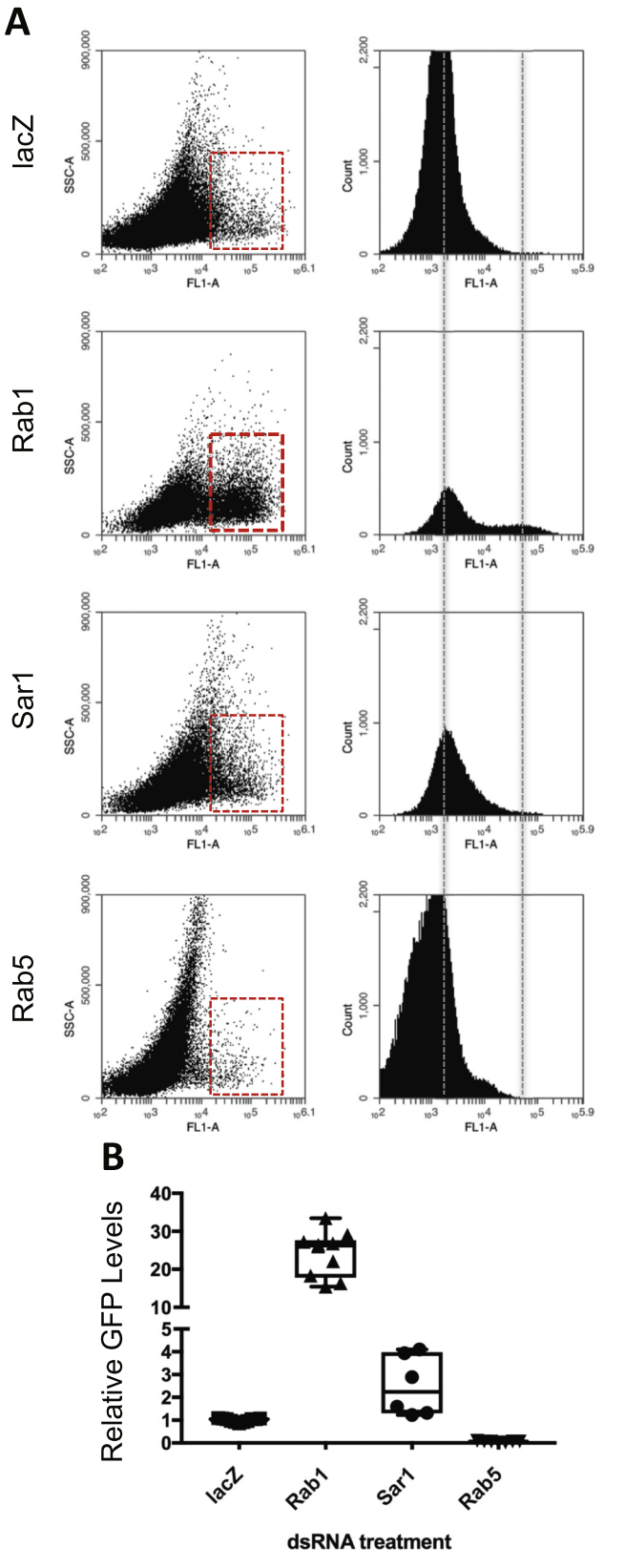

(caption on next page)

Fig. 4. RNAi knockdowns of *Sar1* and *Rab1* genes that enhance reporter baculovirus entry. **A)** Representative images of flow cytometry detection of EGFP positive cells from an analysis of *Sar1* and *Rab1* knockdowns using a modified RNAi assay (see Materials and Methods). EGFP positive populations used for quantification are highlighted by boxes (red dashed lines) in the images on the left (SSC-A/FL1-H plots). Images on the right (count/FL1-A) illustrate the relative proportions of EGFP-labeled vs. unlabeled cells. The dashed line on the left highlights the background mean fluorescence intensity, and the dashed line on the right highlights the mean fluorescence intensity of the EGFP signal. **B)** Entry levels of AcGFP were evaluated by flow cytometry measurements of NLS-EGFP from cells exposed to the indicated dsRNAs in the modified RNAi assay. Data shown are the combined results from three individual wells analyzed in each of three independent assays. LacZ and Rab5 dsRNA treated cells were included as negative and positive controls, respectively.

DNA was then extracted and analyzed by qPCR to determine relative amounts of bound AcMNPV. Viral DNA was measured in reference to cellular DNA (gene *Rp49*). When compared with cells treated with control lacZ dsRNA, we detected no increase in virus bound to cells for which *Rab1* was knocked down, (Fig. 5A, lacZ vs Rab1). Because the entry assay resulted in a > 10-fold increase in EGFP levels when *Rab1* was knocked down, this result indicated that the enhanced EGFP reporter expression in the presence of the *Rab1* knockdown did not result from an enhancement of binding of BV at the plasma membrane. In addition to the *Rab1* result, the observation that the *Rab5* knockdown did not affect virus binding (Fig. 5A, lacZ vs. Rab5), yet dramatically reduced EGFP reporter detection in all our prior assays indicates that the *Rab5* knockdown blocks a step of virus entry beyond initial virus binding to cells.

3.5. Rab1 knockdown does not enhance AcMNPV endocytosis into cells

Because virus binding at the cell surface was not enhanced by the *Rab1* knockdown (Fig. 5A), we next examined the effect of RAB1 depletion on the initial internalization of the virus into the cell from the cell surface. For this experiment we filtered (0.45 μm) the AcMNPV preparation used for binding to remove any large aggregates of virus particles, which might introduce variability to the experiment. Similar to the method used to determine the AcMNPV dose for binding experiments, we first analyzed the filtered AcMNPV preparation and established a linear range for detection of internalization in a dose-dependent manner, using control cells (Fig. 5B). The virus (BV) was bound to cells at 4 °C for 1 h, then removed by washing cells 3x at 4 °C. To initiate entry from the surface, cells were shifted to 27 °C. After 1 h at 27 °C, cells were treated with trypsin (37 °C for 10 min) to remove any virus remaining at the cell surface. Cells were then pelleted, washed 3x in cold PBS, and lysed, then total DNA was analyzed by qPCR to detect virus that was internalized. As a control to ensure that we were detecting DNA only from internalized viral particles, we monitored parallel plates of cells in which virus was bound at 4 °C, but not shifted to 27 °C. Following the binding and washing steps, cells were placed at 4 °C (not 27 °C) for 1 h, then treated with trypsin to remove residual virus at the cell surface. As expected, very little viral DNA was detected from these "binding only" controls, confirming that any bound virus remaining at the cell surface was efficiently removed by protease treatment. Relative to control lacZ dsRNA treated cells, we did not detect an increase in intracellular AcMNPV DNA in the presence of a *Rab1* knockdown (Fig. 5C). Thus, in contrast to the 10-fold increase in the EGFP signal observed in the presence of the *Rab1* knockdown, the initial internalization of AcMNPV from the cell surface was not enhanced by the *Rab1* knockdown, indicating that a subsequent subcellular trafficking pathway is likely affected by the *Rab1* knockdown.

We also monitored virus internalization into Rab5 dsRNA treated cells (for which cell surface binding was not altered; Fig. 5A) although the *Rab5* knockdown almost completely blocked EGFP reporter virus activity. We found that Rab5 dsRNA treated cells did not have a reduced ability to internalize virus. This indicates that the observed reduction of the EGFP reporter in the presence of a *Rab5* knockdown, also likely results from impacts on steps following the initial internalization of AcMNPV BV.

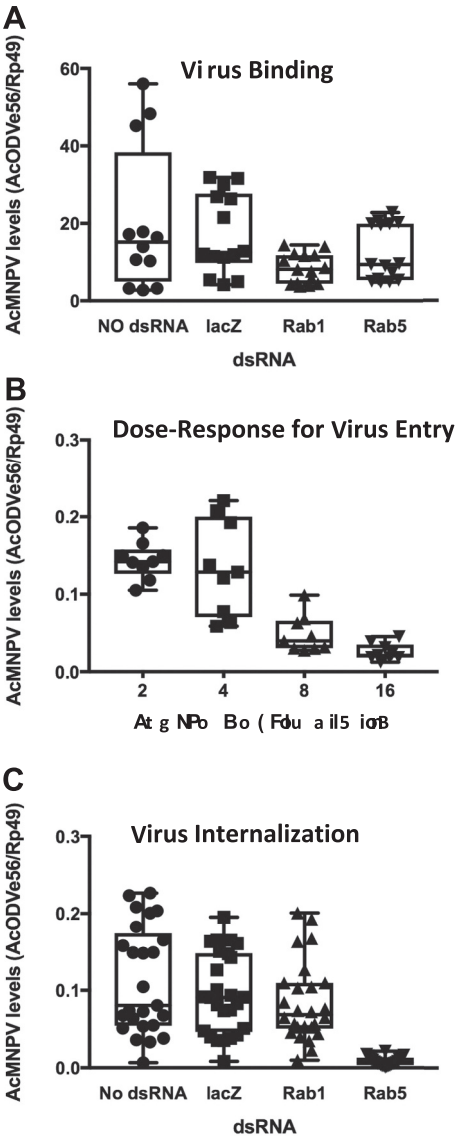

Fig. 5. Analysis of AcMNPV binding and endocytosis. **A)** For each dsRNA knockdown, AcMNPV BV was bound to an equal number of cells for 1 h on ice. Excess unbound virus was removed by washing cells 3x with cold PBS, then total DNA was isolated and viral DNA was measured by qPCR. Results shown comprise two replicate samples for each dsRNA treatment from three independent experiments. **B)** Dose-response for virus entry. To validate quantitative detection of AcMNPV BV internalized by endocytosis, two-fold dilutions of the AcMNPV BV preparation were incubated on cells previously treated with lacZ dsRNA. After removing unbound virus, cells were shifted to 27 °C for 1 h to permit virus entry. To remove any virus remaining at the cell surface, cells were treated with trypsin and washed, then total DNA was isolated from cells, and internalized virus was measured by qPCR detection of viral DNA. Data shown are three replicate samples from three independent experiments. **C)** To analyze virus internalization in the presence of *Rab1* and *Rab5* knockdowns, AcMNPV BV was bound to equal numbers of cells (on ice) that were previously incubated with the indicated dsRNAs. Cells were treated as described in (B) above, and internalized virus was measured by qPCR detection of internalized viral DNA. Data shown comprise triplicate samples for each dsRNA treatment from three independent experiments.

3.6. Knockdown of core autophagy genes does not enhance AcMNPV entry

In addition to its roles in ER-Golgi transport, RAB1 has also been shown to play a role in autophagy in mammalian and insect cells. RAB1 is known to be involved in autophagosome formation (Huang et al., 2011; Kakuta et al., 2017; Zoppino et al., 2010), a process important in cellular immunity to viruses (Rey-Jurado et al., 2015). Thus, we hypothesized that the increased efficiency of AcGFP virus entry in the presence of a *Rab1* knockdown may result from an effect on components of the autophagy pathway that have anti-viral roles. To test this hypothesis, we examined AcGFP virus entry in the presence of RNAi knockdowns of core autophagy genes *Atg1*, *Atg2*, *Atg8a*, and *Atg9*. We detected no increase in AcGFP entry into cells treated with dsRNA targeting any of these genes (Fig. S2A). Knockdowns of *Atg1* and *Atg8a* were confirmed by qRT-PCR and immunoblot analysis, respectively (Fig. S2B and S2C). Thus, the results from knockdowns of core autophagy genes suggest that enhanced AcGFP entry in the *Rab1* knockdown likely did not result from an effect on autophagy.

4. Discussion

To identify cellular proteins and pathways involved in AcMNPV BV entry into cells, we developed a semi-high-throughput RNAi screen. For this screen, a set of 86 host genes was targeted for RNAi knockdowns in *Drosophila* cells. Following RNAi knockdown of each candidate gene, cells were infected with a replication-incompetent recombinant baculovirus (AcGFP) expressing an NLS-EGFP reporter, and cells were screened for reporter activity as a measure of virus entry. In this RNAi screen (which targeted factors known to be involved in vesicular transport), we identified 24 genes that negatively impacted EGFP levels in cells infected with the reporter virus. Of these 24 genes, 8 showed dramatically reduced reporter EGFP expression. These genes included *Vps1*, *Vps4*, *Vps32* and *Vps74*, *Rab3*, *Rab5*, *Rab7* and *Rab8*, *clathrin AP-1–2beta*, and *Arf4*. Some of the most dramatic effects resulted from knockdowns of *Rab5*, *Rab7*, *Vps1* and *Vps74*, each of which reduced reporter detection by more than 80%. Many of these genes are known to be important for endocytosis or the endolysosomal system, consistent with the observed effects on virus uptake into cells and/or release of nucleocapsids from endosomes. For example, VPS74 is a PI4P-binding protein that interacts with ER-Golgi anterograde trafficking of betaCOP-coated vesicles (Tu et al., 2012). Although the receptor for the baculovirus budded virus has not been clearly identified, virions are presumed to bind to a common component of membranes of numerous cell types since baculoviruses enter many cell types, independently of whether cells are permissive for replication by the virus (Airenne et al., 2003; Dong and Blissard, 2012; Kost and Condreay, 2002; Shoji et al., 1997). VPS74 depletion may affect PI4P regulated protein and/or lipid trafficking, possibly altering virion-membrane interactions or endosomal trafficking necessary for BV entry. VPS1 is a dynamin homologue with GTPase activity (Obar et al., 1990; Vater et al., 1992) that has been associated with membrane invagination at the sites of endocytosis *in yeast* (Rooij et al., 2010). Because baculoviruses enter insect and mammalian cells by clathrin-mediated endocytosis (Volkman Goldstein 1985, Long, 2006), RNAi-mediated VPS1 depletion may limit initial or subsequent steps in endocytosis of the AcGFP reporter virus into cells.

RAB5 is required for transport and fusion of plasma membrane-derived vesicles to early endosomes (Bucci et al., 1992) and for fusion among early endosomes (Meresse et al., 1999). RAB5 depletion or functional inhibition has previously been shown to block infection by several other enveloped viruses (reviewed in (Sieczkarski and Whittaker, 2002)). RAB7 in contrast, is associated with late endosomes and is involved in trafficking from early to late endosomes, and from late endosome to lysosomes. In some viruses, virions escape from early endosomes and do not appear to require late endosome trafficking. In those cases, *Rab5* disruption prevents entry while *Rab7* disruption does not. Because we found that RNAi knockdowns of both *Rab5* and *Rab7* substantially reduced detection of the EGFP reporter, this suggests that late endosomes and possibly lysosomes are necessary for AcMNPV BV entry. This is consistent with the low pH threshold (around pH 5.5) for triggering membrane fusion by the baculovirus GP64 membrane fusion protein, and likely release of nucleocapsids from late endosomes (Blissard and Wenz, 1992; Monsma and Blissard, 1995).

Less dramatic in magnitude, knockdowns of *Vps4*, *Vps23*, *Vps11* and *Vps32* also markedly reduced reporter AcGFP detection to about 50% of the control. A dominant negative form of VPS4 was previously shown to block transport of baculovirus nucleocapsids into the nuclei of lepidopteran host cells (*S. frugiperda*) (Li and Blissard, 2012) although the specific step inhibited was not determined. The ATPase activity of VPS4 is required for disassembling and recycling ESCRT III filaments, which are composed largely of VPS32 (SNF7p), a subunit of the ESCRT III complex. The ESCRT III complex mediates scission of newly formed vesicles in intracellular compartments called multivesicular bodies (Shen et al., 2014) (reviewed in (Schmidt and Teis, 2012)). The observation that depletion of *Vps32* and *Vps4* reduced baculovirus entry in the current study is also consistent with prior and recent studies of the importance of certain ESCRT pathway components in BV entry (Li and Blissard, 2012; Yue et al., 2018). VPS23 (Tsg101) is an ESCRT I subunit required for directing assembly of the ESCRT I complex and is the portion of ESCRT I that recognizes ubiquitinated cargo destined for endolysosomal degradation (Katzmann et al., 2001). VPS11 is a component of the HOPS complex that is needed for early to late endosome maturation and endosomal fusion with autophagosomes and lysosomes (Chirivino et al., 2011; Wartosch et al., 2015). Therefore, since knockdowns of *Vps4*, *Vps11*, *Vps23* and *Vps32* limited baculovirus reporter activity, the complexity and specificity of cellular pathways utilized during budded virus entry are beginning to come into focus.

Recently, several VPS/ESCRT III proteins were identified as important for baculovirus (AcMNPV) entry into and transport within permissive cells of lepidopteran hosts *Spodoptera frugiperda* (Sf9 cells) and *Trichoplusia ni* (High5 cells) (Yue et al., 2018). In that study, both RNAi and dominant negative protein constructs were used to disrupt vesicular trafficking and the following ESCRT III components were identified as important for BV entry: VPS2B, VPS4, VPS20, VPS24, VPS26, VPS60 and VPS32. As described above, data from the current screen (which assessed reporter baculovirus entry into *Drosophila* cells) is in good general agreement with data from AcMNPV entry into lepidopteran cells (Yue et al., 2018). We noted several differences also. One observed difference is that *Vps23* (*Tsg101*) knockdown was moderately inhibitory (45% reduction in EGFP positive cells) to reporter virus entry into *Drosophila* cells in the current study, whereas no effect on virus entry into lepidopteran cells was observed in the prior study (Yue et al., 2018). Also, whereas the current screen with *Drosophila* cells did not result in reduced entry upon knockdown of *Vps2B*, *Vps20* or *Vps24*, AcMNPV entry into Sf9 and High5 cells was significantly reduced when those components were disrupted by RNAi or DN protein overexpression (Yue et al., 2018). It is currently unclear whether the differences observed between the current and prior study (Yue et al., 2018) in *Drosophila* and lepidopteran cells, respectively, indicate differences in entry mechanisms or pathways, or whether this reflects differences in the experimental systems. While *Drosophila* differs substantially in size and habitat from permissive lepidopteran hosts such as *S. frugiperda* and *T. ni*, the genomes of these permissive insect species have substantial similarities with the *Drosophila* genome. For example, the *T. ni* genome has an estimated 14,374 protein coding genes (Chen et al., In press; Fu et al., 2018) and the *D. melanogaster* genome has approximately 13,883 protein coding genes (Hoskins et al., 2015). Lepidopteran species (such as *T. ni, M. sexta*, *B. mori*, and *D. plexippus*) encode orthologs of most genes found in the *Drosophila melanogaster* genome (Chen et al., In Press; Kanost et al., 2016; Li and Blissard, 2015; Zhan et al., 2011). For *Drosophila* gene knockdowns that significantly altered AcGFP entry in the current study, orthologs from permissive

hosts *T. ni* and *S. frugiperda* were identified by reciprocal BLAST analysis and are listed in Table S4. All 28 of the *Drosophila* genes that we identified as important for AcGFP entry were identified in the *T. ni* transcriptome and all but two (Rab2 and Rab3) were identified from the *S. frugiperda* genome. Therefore, the current study in *Drosophila* cells reveals specific cellular proteins that may form the basis for a generalized entry pathway for AcMNPV BV.

An unexpected but important result from the current RNAi screen was the increase in EGFP reporter detection from four of the cellular gene knockdowns (*Vps2*, *Rab1*, *betaCOP*, and *Sar1*). This suggested that these proteins may play roles in restricting either binding, cellular uptake, or intracellular transport of virions or nucleocapsids to the nucleus. We were particularly interested in the *Rab1* knockdown, which increased the EGFP reporter by more than 10-fold relative to control cells. Although the relevant step in entry was not identified, further analysis indicated that virion binding and internalization were not affected by the *Rab1* knockdown, suggesting that the effect was due to one or more of the downstream steps such as: vesicular transport, vesicle-virion fusion, actin propulsion of nucleocapsids, or nuclear entry. Also, although unlikely, nucleocapsid uncoating or reporter gene transcription or translation could also be affected, and cannot be formally eliminated.

A major function of RAB1 is the regulation of anterograde vesicle transport from ER-to-Golgi, which if blocked, may affect secretion and/or surface display of some glycoproteins (Plutner et al., 1991, 1990). RAB1 also plays a role in biogenesis of autophagosomes (Huang et al., 2011; Zirin and Perrimon, 2010; Zoppino et al., 2010). Autophagy also restricts infection by a variety of intracellular pathogens (a process termed xenophagy) including HSV-1 (Kirkegaard et al., 2004; Smith and de Harven, 1978), another large enveloped nuclear DNA virus. The HSV-1 ICP34.5 protein targets the proautophagic activity of the Beclin1 protein (ATG6 in yeast) and blocks HSV-1 induced autophagy in neurons, thus enabling viral replication to levels that cause neurovirulence (Orvedahl et al., 2007). AcMNPV transduction of non-permissive mammalian (HeLa) cells was also reported to be negatively impacted by autophagy since pre-treatment of cells with 3-methyladenine (3-MA), a PI3K inhibitor that decreases autophagosome biogenesis, was shown to increase viral transduction efficiency (Liu et al., 2014; Wei et al., 2012). However, 3-MA may also result in a variety of pleiotropic effects in cells, so we assessed baculovirus transduction based on EGFP reporter expression, in the presence of RNAi-mediated knockdown of several core autophagy genes. When we examined effects of RNAi knockdowns of the core autophagy genes *Atg1*, *Atg2*, *Atg8a* and *Atg9*, we observed no increase in EGFP reporter detection. We therefore conclude that enhanced viral entry resulting from the *Rab1* knockdown was unlikely to be caused by an inhibition of autophagy.

RAB1 has also been described as a tethering factor for the WASP homologue associated with actin, membranes, and microtubules (WHAMM) that mediates polymerization of actin, but which limits f-actin nucleation (Russo et al., 2016). In this context RAB1 was shown to stimulate assembly of WHAMM-associated actin containing structures in mammalian fibroblasts. However, RAB1 binding to WHAMM blocked nucleation of f-actin synthesis. Baculovirus nucleocapsids contain an f-actin nucleating protein (p78/83) that induces actin polymerization to propel viral nucleocapsids in the cytoplasm and to drive transit across the nuclear pore in insect and vertebrate cells (Au et al., 2013, 2016; Mueller et al., 2014; Ohkawa et al., 2010). Thus, knockdown of *Rab1* may possibly affect actin polymerization associated with propulsion of the nucleocapsids in the cytoplasm, or their movement across the nuclear pore. It is also interesting to note that VPS4 and several ESCRT-III proteins were reported to be associated with the assembly and perhaps maintenance of the nuclear pore complex (Webster et al., 2014) and it is therefore possible that the observed effect of some knockdowns may result from effects on nuclear entry by the nucleocapsid. Proteins such as ESCRT complex components and Rab proteins serve a complex variety of roles in the cell (Bhuin and Roy, 2014; Goody et al., 2017; Hurley, 2015) and understanding the precise mechanisms by which knockdowns or dominant negative constructs inhibit or enhance virus entry will be an ongoing challenge in virology and cell biology.

Acknowledgements

We thank Sara Cherry for providing DL1 cells, and are grateful to Ana Rita Rebelo for assistance with qPCR, and to Peter Nagy for discussions on autophagy. We also thank Gabor Juhasz for providing the ATG8 antiserum. This work was supported by NSF grants 1354421 and 1653021 to GWB and NB, and USDA grant 2015-67013-23281 to GWB.

Appendix A. Supporting information

Supplementary data associated with this article can be found in the online version at doi:10.1016/j.virol.2018.10.022

References

Airenne, K.J., Hu, Y.C., Kost, T.A., Smith, R.H., Kotin, R.M., Ono, C., Matsuura, Y., Wang, S., Yla-Herttuala, S., 2013. Baculovirus: an insect-derived vector for diverse gene transfer applications. Mol. Ther. 21, 739–749.

Airenne, K.J., Peltomaa, E., Hytonen, V.P., Laitinen, O.H., Yla-Herttuala, S., 2003. Improved generation of recombinant baculovirus genomes in Escherichia coli. Nucleic Acids Res. 31, e101.

Au, S., Wu, W., Pante, N., 2013. Baculovirus nuclear import: open, nuclear pore complex (NPC) sesame. Viruses 5, 1885–1900.

Au, S., Wu, W., Zhou, L., Theilmann, D.A., Pante, N., 2016. A new mechanism for nuclear import by actin-based propulsion used by a baculovirus nucleocapsid. J. Cell Sci. 129, 2905–2911.

Barrowman, J., Bhandari, D., Reinisch, K., Ferro-Novick, S., 2010. TRAPP complexes in membrane traffic: convergence through a common Rab. Nat. Rev. Mol. Cell Biol. 11, 759–763.

Bhuin, T., Roy, J.K., 2014. Rab proteins: the key regulators of intracellular vesicle transport. Exp. Cell Res. 328, 1–19.

Birmingham, A., Selfors, L.M., Forster, T., Wrobel, D., Kennedy, C.J., Shanks, E., Santoyo-Lopez, J., Dunican, D.J., Long, A., Kelleher, D., Smith, Q., Beijersbergen, R.L., Ghazal, P., Shamu, C.E., 2009. Statistical methods for analysis of high-throughput RNA interference screens. Nat. Methods 6, 569–575.

Blissard, G.W., Wenz, J.R., 1992. Baculovirus GP64 envelope glycoprotein is sufficient to mediate pH dependent membrane fusion. J. Virol. 66, 6829–6835.

Bucci, C., Parton, R.G., Mather, I.H., Stunnenberg, H., Simons, K., Hoflack, B., Zerial, M., 1992. The small GTPase rab5 functions as a regulatory factor in the early endocytic pathway. Cell 70, 715–728.

Chen, W., Yang, X., Tetreau, G., Song, X., Coutu, C., Hegedus, D., Blissard, G., Fei, Z., Wang, P., In Press. A high-quality chromosome-level genome assembly of a generalist herbivore, *Trichoplusia ni*. Mol. Ecol. Resour.

Cherry, S., 2008. Genomic RNAi screening in *Drosophila* S2 cells: what have we learned about host-pathogen interactions? Curr. Opin. Microbiol. 11, 262–270.

Chirivino, D., Del Maestro, L., Formstecher, E., Hupe, P., Raposo, G., Louvard, D., Arpin, M., 2011. The ERM proteins interact with the HOPS complex to regulate the maturation of endosomes. Mol. Biol. Cell 22, 375–385.

Dong, S., Blissard, G.W., 2012. Functional analysis of the *Autographa californica* multiple nucleopolyhedrovirus GP64 terminal fusion loops and interactions with membranes. J. Virol. 86, 9617–9628.

Felberbaum, R.S., 2015. The baculovirus expression vector system: a commercial manufacturing platform for viral vaccines and gene therapy vectors. Biotechnol. J. 10, 702–714.

Fu, Y., Yang, Y., Zhang, H., Farley, G., Wang, J., Quarles, K.A., Weng, Z., Zamore, P.D., 2018. The genome of the Hi5 germ cell line from Trichoplusia ni, an agricultural pest and novel model for small RNA biology. eLife 7, e31628.

Goody, R.S., Muller, M.P., Wu, Y.W., 2017. Mechanisms of action of Rab proteins, key regulators of intracellular vesicular transport. Biol. Chem. 398, 565–575.

Hefferon, K., Oomens, A., Monsma, S., Finnerty, C., Blissard, G.W., 1999. Host cell receptor binding by baculovirus GP64 and kinetics of virion entry. Virology 258, 455–468.

Hoskins, R.A., Carlson, J.W., Wan, K.H., Park, S., Mendez, I., Galle, S.E., Booth, B.W., Pfeiffer, B.D., George, R.A., Svirskas, R., Krzywinski, M., Schein, J., Accardo, M.C., Damia, E., Messina, G., Mendez-Lago, M., de Pablos, B., Demakova, O.V., Andreyeva, E.N., Boldyreva, L.V., Marra, M., Carvalho, A.B., Dimitri, P., Villasante, A., Zhimulev, I.F., Rubin, G.M., Karpen, G.H., Celniker, S.E., 2015. The Release 6 reference sequence of the Drosophila melanogaster genome. Genome Res. 25, 445–458.

Hu, Y.C., 2010. Baculovirus: a promising vector for gene therapy? Curr. Gene Ther. 10, 167.

Huang, J., Birmingham, C.L., Shahnazari, S., Shiu, J., Zheng, Y.T., Smith, A.C., Campellone, K.G., Heo, W.D., Gruenheid, S., Meyer, T., Welch, M.D., Ktistakis, N.T., Kim, P.K., Klionsky, D.J., Brumell, J.H., 2011. Antibacterial autophagy occurs at PI(3)P-enriched domains of the endoplasmic reticulum and requires Rab1 GTPase. Autophagy 7, 17–26.

Hurley, J.H., 2015. ESCRTs are everywhere. EMBO J.

Kakuta, S., Yamaguchi, J., Suzuki, C., Sasaki, M., Kazuno, S., Uchiyama, Y., 2017. Small GTPase Rab1B is associated with ATG9A vesicles and regulates autophagosome formation. FASEB J. 31, 3757–3773.
Kalesnykas, G., Kokki, E., Alasaarela, L., Lesch, H.P., Tuulos, T., Kinnunen, K., Uusitalo, H., Airenne, K., Yla-Herttuala, S., 2017. Comparative study of adeno-associated virus, adenovirus, Baculovirus and Lentivirus vectors for gene therapy of the eyes. Curr. Gene Ther.
Kanost, M.R., Arrese, E.L., Cao, X., Chen, Y.-R., Chellapilla, S., Goldsmith, M., Grosse-Wilde, E., Heckel, D.G., Herndon, N., Jiang, H., Papanicolaou, A., Qu, J., Soulages, J.L., Vogel, H., Walters, J., Waterhouse, R.M., Ahn, S.-J., Almeida, F.C., An, C., Aqrawi, P., Bretschneider, A., Bryant, W.B., Bucks, S., Chao, H., Chevignon, G., Christen, J.M., Clarke, D.F., Dittmer, N.T., Ferguson, L.C.F., Garavelou, S., Gordon, K.H.J., Gunaratna, R.T., Han, Y., Hauser, F., He, Y., Heidel-Fischer, H., Hirsh, A., Hu, Y., Jiang, H., Kalra, D., Klinner, C., König, C., Kovar, C., Kroll, A.R., Kuwar, S.S., Lee, S.L., Lehman, R., Li, K., Li, Z., Liang, H., Lovelace, S., Lu, Z., Mansfield, J.H., McCulloch, K.J., Mathew, T., Morton, B., Muzny, D.M., Neunemann, D., Ongeri, F., Pauchet, Y., Pu, L.-L., Pyrousis, I., Rao, X.-J., Redding, A., Roesel, C., Sanchez-Gracia, A., Schaack, S., Shukla, A., Tetreau, G., Wang, Y., Xiong, G.-H., Traut, W., Walsh, T.K., Worley, K.C., Wu, D., Wu, W., Wu, Y.-Q., Zhang, X., Zou, Z., Zucker, H., Briscoe, A.D., Burmester, T., Clem, R.J., Feyereisen, R., Grimmelikhuijzen, C.J.P., Hamodrakas, S.J., Hansson, B.S., Huguet, E., Jermiin, L.S., Lan, Q., Lehman, H.K., Lorenzen, M., Merzendorfer, H., Michalopoulos, I., Morton, D.B., Muthukrishnan, S., Oakeshott, J.G., Palmer, W., Park, Y., Passarelli, A.L., Rozas, J., Schwartz, L.M., Smith, W., Southgate, A., Vilcinskas, A., Vogt, R., Wang, P., Werren, J., Yu, X.-Q., Zhou, J.-J., Brown, S.J., Scherer, S.E., Richards, S., Blissard, G.W., 2016. Multifaceted Biological Insights from a Draft Genome Sequence of the Tobacco Hornworm Moth, *Manduca sexta*. Insect Biochem. Mol. Biol. 76, 118–147.
Katzmann, D.J., Babst, M., Emr, S.D., 2001. Ubiquitin-dependent sorting into the multivesicular body pathway requires the function of a conserved endosomal protein sorting complex, ESCRT-I. Cell 106, 145–155.
Kirkegaard, K., Taylor, M.P., Jackson, W.T., 2004. Cellular autophagy: surrender, avoidance and subversion by microorganisms. Nat. Rev. Microbiol. 2, 301–314.
Kost, T.A., Condreay, J.P., 2002. Recombinant baculoviruses as mammalian cell gene-delivery vectors. Trends Biotechnol. 20, 173–180.
Kukkonen, S.P., Airenne, K.J., Marjomaki, V., Laitinen, O.H., Lehtolainen, P., Kankaanpaa, P., Mahonen, A.J., Raty, J.K., Nordlund, H.R., Oker-Blom, C., Kulomaa, M.S., Yla-Herttuala, S., 2003. Baculovirus capsid display: a novel tool for transduction imaging. Mol. Ther. 8, 853–862.
Li, Z., Blissard, G., 2015. The vacuolar protein sorting genes in insects: a comparative genome view. Insect Biochem. Mol. Biol. 62, 211–225.
Li, Z., Blissard, G.W., 2012. Cellular VPS4 is required for efficient entry and egress of budded virions of *Autographa californica* multiple Nucleopolyhedrovirus. J. Virol. 86, 459–472.
Liu, Y., Joo, K.I., Lei, Y., Wang, P., 2014. Visualization of intracellular pathways of engineered baculovirus in mammalian cells. Virus Res. 181, 81–91.
Long, G., Pan, X., Kormelink, R., Vlak, J.M., 2006. Functional entry of baculovirus into insect and mammalian cells is dependent on clathrin-mediated endocytosis. J. Virol. 80, 8830–8833.
Mansouri, M., Bellon-Echeverria, I., Rizk, A., Ehsaei, Z., Cianciolo Cosentino, C., Silva, C.S., Xie, Y., Boyce, F.M., Davis, M.W., Neuhauss, S.C., Taylor, V., Ballmer-Hofer, K., Berger, I., Berger, P., 2016. Highly efficient baculovirus-mediated multigene delivery in primary cells. Nat. Commun. 7, 11529.
Mansouri, M., Berger, P., 2018. Baculovirus for gene delivery to mammalian cells: past, present and future. Plasmid 98, 1–7.
Mercer, J., Schelhaas, M., Helenius, A., 2010. Virus entry by endocytosis. Annu. Rev. Biochem. 79, 803–833.
Meresse, S., Steele-Mortimer, O., Finlay, B.B., Gorvel, J.P., 1999. The rab7 GTPase controls the maturation of Salmonella typhimurium-containing vacuoles in HeLa cells. EMBO J. 18, 4394–4403.
Monsma, S.A., Blissard, G.W., 1995. Identification of a membrane fusion domain and an oligomerization domain in the baculovirus GP64 envelope fusion protein. J. Virol. 69, 2583–2595.
Mueller, J., Pfanzelter, J., Winkler, C., Narita, A., Le Clainche, C., Nemethova, M., Carlier, M.F., Maeda, Y., Welch, M.D., Ohkawa, T., Schmeiser, C., Resch, G.P., Small, J.V., 2014. Electron tomography and simulation of baculovirus actin comet tails support a tethered filament model of pathogen propulsion. PLoS Biol. 12, e1001765.
O'Reilly, D.R., Miller, L.K., Luckow, V.A., 1992. Baculovirus Expression Vectors, A Laboratory Manual. W. H. Freeman and Co., New York.
Obar, R.A., Collins, C.A., Hammarback, J.A., Shpetner, H.S., Vallee, R.B., 1990. Molecular cloning of the microtubule-associated mechanochemical enzyme dynamin reveals homology with a new family of GTP-binding proteins. Nature 347, 256–261.
Ohkawa, T., Volkman, L.E., Welch, M.D., 2010. Actin-based motility drives baculovirus transit to the nucleus and cell surface. J. Cell Biol. 190, 187–195.
Ohkawa, T., Welch, M.D., 2018. Baculovirus actin-based motility drives nuclear envelope disruption and nuclear egress. Curr. Biol. 28 (2153–2159), e2154.
Orvedahl, A., Alexander, D., Talloczy, Z., Sun, Q., Wei, Y., Zhang, W., Burns, D., Leib, D.A., Levine, B., 2007. HSV-1 ICP34.5 confers neurovirulence by targeting the Beclin 1 autophagy protein. Cell Host Microbe 1, 23–35.
Plutner, H., Cox, A.D., Pind, S., Khosravi-Far, R., Bourne, J.R., Schwaninger, R., Der, C.J., Balch, W.E., 1991. Rab1b regulates vesicular transport between the endoplasmic reticulum and successive Golgi compartments. J. Cell Biol. 115, 31–43.
Plutner, H., Schwaninger, R., Pind, S., Balch, W.E., 1990. Synthetic peptides of the Rab effector domain inhibit vesicular transport through the secretory pathway. EMBO J. 9, 2375–2383.
Rey-Jurado, E., Riedel, C.A., Gonzalez, P.A., Bueno, S.M., Kalergis, A.M., 2015. Contribution of autophagy to antiviral immunity. FEBS Lett. 589, 3461–3470.
Rooij, I.I.S.-d., Allwood, E.G., Aghamohammadzadeh, S., Hettema, E.H., Goldberg, M.W., Ayscough, K.R., 2010. A role for the dynamin-like protein Vps1 during endocytosis in yeast. J. Cell Sci. 123, 3496.
Russo, A.J., Mathiowetz, A.J., Hong, S., Welch, M.D., Campellone, K.G., 2016. Rab1 recruits WHAMM during membrane remodeling but limits actin nucleation. Mol. Biol. Cell 27, 967–978.
Schmidt, O., Teis, D., 2012. The ESCRT machinery. Curr. Biol. 22, R116–R120.
Shen, Q.T., Schuh, A.L., Zheng, Y., Quinney, K., Wang, L., Hanna, M., Mitchell, J.C., Otegui, M.S., Ahlquist, P., Cui, Q., Audhya, A., 2014. Structural analysis and modeling reveals new mechanisms governing ESCRT-III spiral filament assembly. J. Cell Biol. 206, 763–777.
Shoji, I., Aizaki, H., Tani, H., Ishii, K., Chiba, T., Saito, I., Miyamura, T., Matsuura, Y., 1997. Efficient gene transfer into various mammalian cells, including non-hepatic cells, by baculovirus vectors. J. Gen. Virol. 78, 2657–2664.
Sieczkarski, S.B., Whittaker, G.R., 2002. Dissecting virus entry via endocytosis. J. Gen. Virol. 83, 1535–1545.
Smith, J.D., de Harven, E., 1978. Herpes simplex virus and human cytomegalovirus replication in WI-38 cells. III. cytochemical localization of lysosomal enzymes in infected cells. J. Virol. 26, 102–109.
Takats, S., Nagy, P., Varga, A., Pircs, K., Karpati, M., Varga, K., Kovacs, A.L., Hegedus, K., Juhasz, G., 2013. Autophagosomal Syntaxin17-dependent lysosomal degradation maintains neuronal function in Drosophila. J. Cell Biol. 201, 531–539.
Tu, L., Chen, L., Banfield, D.K., 2012. A conserved N-terminal arginine-motif in GOLPH3-family proteins mediates binding to coatomer. Traffic 13, 1496–1507.
Vater, C.A., Raymond, C.K., Ekena, K., Howald-Stevenson, I., Stevens, T.H., 1992. The VPS1 protein, a homolog of dynamin required for vacuolar protein sorting in Saccharomyces cerevisiae, is a GTPase with two functionally separable domains. J. Cell Biol. 119, 773–786.
Volkman, L.E., Goldsmith, P.A., 1985. Mechanism of neutralization of budded *Autographa californica* nuclear polyhedrosis virus by a monoclonal antibody: inhibition of entry by adsorptive endocytosis. Virology 143, 185–195.
Wang, P., Hammer, D.A., Granados, R.R., 1997. Binding and fusion of *Autographa californica* nucleopolyhedrovirus to cultured insect cells. J. Gen. Virol. 78, 3081–3089.
Wartosch, L., Gunesdogan, U., Graham, S.C., Luzio, J.P., 2015. Recruitment of VPS33A to HOPS by VPS16 Is Required for Lysosome Fusion with Endosomes and Autophagosomes. Traffic 16, 727–742.
Webster, B.M., Colombi, P., Jager, J., Lusk, C.P., 2014. Surveillance of nuclear pore complex assembly by ESCRT-III/Vps4. Cell 159, 388–401.
Wei, W., Gai, Z., Ai, H., Wu, W., Yang, Y., Peng, J., Hong, H., Li, Y., Liu, K., 2012. Baculovirus infection triggers a shift from amino acid starvation-induced autophagy to apoptosis. PLoS One 7, e37457.
Wickham, T., Granados, R.R., Wood, H.A., Hammer, D.A., Shuler, M.L., 1990. General analysis of receptor-mediated viral attachment to cell surfaces. Biophys. J. 58, 1501–1516.
Wickham, T.J., Shuler, M.L., Hammer, D.A., Granados, R.R., Wood, H.A., 1992. Equilibrium and kinetic analysis of *Autographa californica* Nuclear Polyhedrosis Virus attachment to different insect cell lines. J. Gen. Virol. 73, 3185–3194.
Yasunaga, A., Hanna, S.L., Li, J., Cho, H., Rose, P.P., Spiridigliozzi, A., Gold, B., Diamond, M.S., Cherry, S., 2014. Genome-wide RNAi screen identifies broadly-acting host factors that inhibit Arbovirus infection. PLoS Pathog. 10, e1003914.
Yue, Q., Yu, Q., Yang, Q., Xu, Y., Guo, Y., Blissard, G.W., Li, Z., 2018. Distinct roles of cellular ESCRT-I and ESCRT-III proteins in efficient entry and egress of budded virions of autographa californica multiple nucleopolyhedrovirus. J. Virol. 92 (e01636-01617).
Zhan, S., Merlin, C., Boore, J.L., Reppert, S.M., 2011. The monarch butterfly genome yields insights into long-distance migration. Cell 147, 1171–1185.
Zhang, J.H., Chung, T.D., Oldenburg, K.R., 1999. A simple statistical parameter for use in evaluation and validation of high throughput screening assays. J. Biomol. Screen 4, 67–73.
Zirin, J., Perrimon, N., 2010. *Drosophila* as a model system to study autophagy. Semin Immunopathol. 32, 363–372.
Zoppino, F.C., Militello, R.D., Slavin, I., Alvarez, C., Colombo, M.I., 2010. Autophagosome formation depends on the small GTPase Rab1 and functional ER exit sites. Traffic 11, 1246–1261.